METAL-CENTRIC PERSPECTIVE ON CHONDRULE FORMATION AND DEFORMATION: ORIENTATION AND CHEMICAL ANALYSIS OF METAL RIMS AND NODULES IN ACFER 139 (CR2).

E. J. Crapster-Pregont[1,2], W. H. Towbin[3], and D. S. Ebel[1,2]. [1]Lamont-Doherty Earth Observatory, Columbia University, Palisades, NY, 10964, USA (ellencp@ldeo.columbia.edu). [2]Dept. of Earth and Planetary Science, American Museum of Natural History, New York, NY, 10024, USA (debel@amnh.org). [3]Microscopy and Imaging Facility, American Museum of Natural History, New York, NY, 10024, USA (htowbin@amnh.org).

Introduction: Chondrites and their components are physical representations of chemical reservoirs and the dynamic history of the early Solar System. Within the types of chondrites, carbonaceous Renazzo-types (CR) have experienced minimal alteration and contain high modal abundances of chondrules [1]. Many of these chondrules contain metal, as interior nodules and/or rims, which enhances their applicability toward constraining chondrule formation hypotheses [2].

This study is a continuation of [3-4], an investigation of metal nodules in chondrules of the Saharan find Acfer 139 (Fig. 1). The multi-layered chondrule in this section of Acfer 139 (Fig. 1; chondrule A) was previously described by [5-6]. This metal-centric study builds on previous studies of metal layers in CR chondrules [e.g. 7-14] by further examining the relationship between chemical and textural characteristics within and among metal nodules in chondrules.

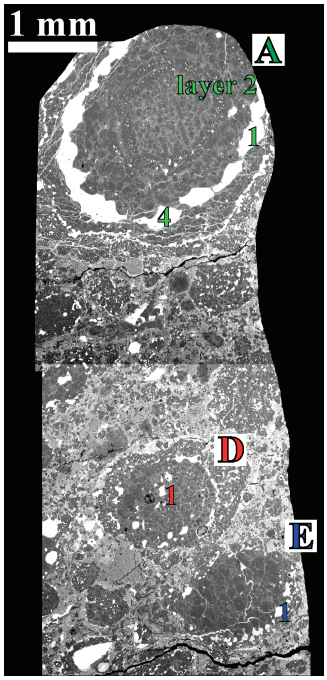

Figure 1: Partial BSE of Acfer 139 surface used in this study. Lightest regions correspond to location of metal. Select chondrules and metal nodules are labeled and image orientation, chemical, and grain information are compared in Fig. 2.

Method: A serial thick section of Acfer 139 (AMNH 4793-t2-ps5B2) was highly polished using a series of grits and slurries finishing with 0.05µm colloidal silica [3]. No carbon coat was initially applied but a thin coat was applied after initial EBSD analysis to facilitate chemical analysis.

Orientation analysis was conducted using an EDAX DigiView IV electron backscatter diffractometer attached to a Zeiss variable pressure EVO 60 scanning electron microscope. The EDAX OIM software was used to process the diffraction data and produced a range of information including grain orientation maps. The AMNH Cameca SX100 electron microprobe (15kV accelerating voltage, 20nA current, 1µm beam size) was used to map elements and to collect single point and multi-point transects of select metal nodules within the section analyzed.

Results: Select, preliminary results are shown in Figure 2: element abundance (FeNiCo=RGB composite), orientation (inverse pole figure), and metal grains (number of grains and relative size of grains). Metal nodules from rims include (Fig. 1): two nodules (1 and 4) from the 2nd metal layer in chondrule A, and nodule 1 from chondrule E. An interior metal nodule (1) in chondrule D is also included for comparison. These results demonstrate the variation in the character of metal nodules within chondrule interiors and rims.

Fe, Ni, and Co are the major elements in these metal nodules. The RGB composite (Fig. 2; 2nd image in each row) highlights the differences in element distributions between nodules. Some display regions of Ni enrichment. The inverse pole figure (Fig. 2; 3rd image in row) is false colored to distinguish between points of different orientation (see legend in image). There are clear, sub-parallel, lamellar-like features transecting many of the nodules. Each metal nodule contains different numbers of grains (Fig. 2; different colors within 4th image in row) and grain sizes are independent of metal nodule location within the chondrule or overall nodule size.

Discussion: The observed Ni heterogeneity (Fig. 2 A.1 and A.4) is not a product of sample preparation as it is not uniformly observed and as the metal nodules exhibit minimal topographic variation [3]. EMP measured transects will verify the presence or absence of major element variation across each metal nodule. Comparison of the occurrence of this elemental variation with the position of the nodule within and among chondrules will allow determination of whether the

metal and chondrules experienced a shared history from initial chemical reservoir to subsequent alteration.

The lamellae-like features are twins based on their orientation difference relative to the rest of each grain (Fig. 2). A more detailed comparison of the twins and the elemental heterogeneity, present in Ni in some metal nodules, will aid in determining whether these twins are exsolution of taenite [15], shock-induced Neumann lines [16], or polysynthetic twins in kamacite. All of these explanations have significant implications for the formation and deformation history of the metal nodules and the associated chondrules in CR chondrites.

There is significantly more information that can be extracted from the EBSD data in addition to the inverse pole figure (orientation) and grain designation images shown in Fig. 2. This information will be produced using features within the EDAX OIM software and will aid in determining the extent of deformation that the chondrule metal experienced. Constraining deformation and its relationship to chemistry could assist in differentiating between pre- and post-accretion events affecting CR chondrites.

Further analysis of this dataset will reveal information on whether multiple chemical reservoirs existed for the metal nodules, reveal similarities of processing history among metal nodules, and allow evaluation of existing chondrule metal layer formation hypotheses [e.g. 11-14]. Overall, metal nodules, both interior and rim, and comparison with chondrule type, add constraints to the conditions of sequential formation of igneous chondrules in the early Solar System.

Acknowledgements: This research is supported by NASA Emerging Worlds grant NNX16AD37G (DSE) and the National Science Foundation Graduate Research Fellowship Program (DGE-11-44155) (ECP).

References: [1] Weisberg M.K. et al. (2006) *Meteorites and the Early Solar System II, Univ. Arizona Press*, 19-52. [2] Wood J.A. 1963. *Icarus*, *2*, 152-180. [3] Crapster-Pregont E.J. et al. (2015). *LPS XLVI*, Abstract #1561. [4] Crapster-Pregont E.J. et al. (2015) *Meteor. Planet. Sci. Suppl., 50,* A96. [5] Ebel D.S. and Downen M.R. (2011) *Meteor. Planet. Sci. Suppl., 46,* A62. [6] Hobart K.K. et al. (2015) LPS XLVI, Abstract #1978. [7] Kong P. et al. (1999) *Geochim. Cosmochim. Acta*, *63*, 2637-2652. [8] Lee M. S. et al. (1992) *GCA*, 56, 2521-2533. [9] Zanda B. et al. (2002) *GCA*, *66*, A869. [10] Kong P. and Palme H. (1999) *GCA*, *63*, 3673-3682. [11] Connolly H. C. et al. (2001) *GCA*, *65*, 4567-4588. [12] Campbell A. J. et al. (2005) *In Chondrites and the Protoplanetary Disk*, MNRAS 341, 407-431. [13] Ebel D. S. et al. (2008) *Meteor. Planet. Sci.*, *43*, 725-1740. [14] Wasson J. T. and Rubin A. E. (2010) *GCA*, *74*, 2212-2230. [15] Goldstein J.I. and Michael J.R. (2006) *Meteor. Planet. Sci.*, *41*, 553-570. [16] Ramdohr P. (1973) *The Opaque Minerals in Stony Meteorites, Elsevier*, 245p.

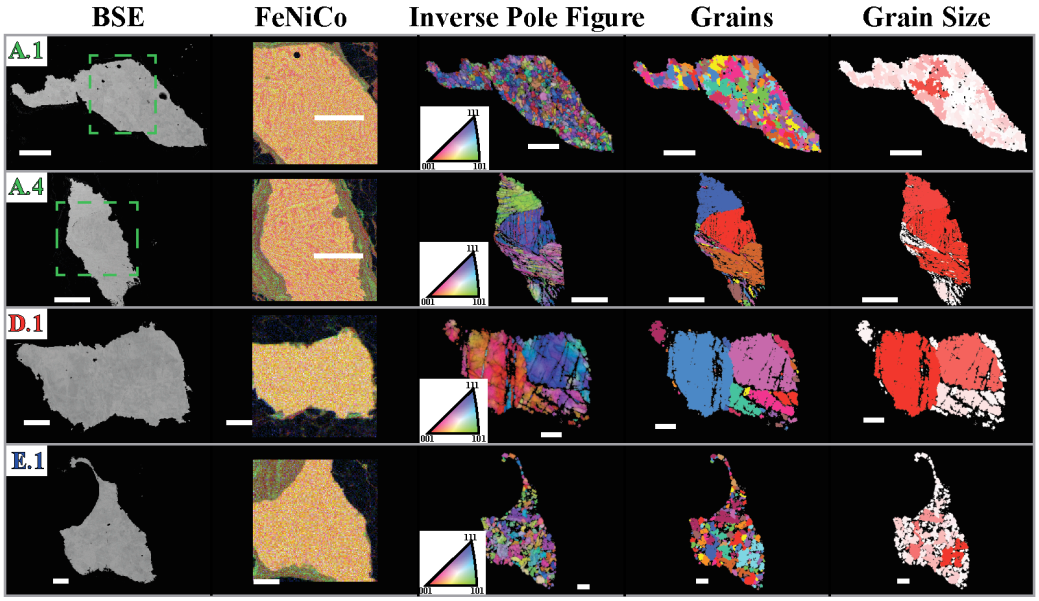

Figure 2: Select results for 4 metal nodules in 3 chondrules considered in this study of chondrule metal of Acfer 139. Results include BSE, three-element x-ray intensity RGB composite (FeNiCo), inverse pole figure and legend (crystallographic orientation), false-colored grain ID, and false-colored by grain size. Dashed outlines in the BSE images denote the location of the high resolution EMP chemical maps. 20μm scale bars are included for reference. Relative locations of the chondrules (letters) and nodules (numbers) are shown in Fig. 1.